General Disclaimer

One or more of the Following Statements may affect this Document

- This document has been reproduced from the best copy furnished by the organizational source. It is being released in the interest of making available as much information as possible.

- This document may contain data, which exceeds the sheet parameters. It was furnished in this condition by the organizational source and is the best copy available.

- This document may contain tone-on-tone or color graphs, charts and/or pictures, which have been reproduced in black and white.

- This document is paginated as submitted by the original source.

- Portions of this document are not fully legible due to the historical nature of some of the material. However, it is the best reproduction available from the original submission.

X-620-77-209
PREPRINT

TMX 71381

CHARGE EXCHANGE LIFETIMES FOR IONS IN THE MAGNETOSPHERE

PAUL H. SMITH
N. K. BEWTRA

JUNE 1977

GSFC
GODDARD SPACE FLIGHT CENTER
GREENBELT, MARYLAND

CHARGE EXCHANGE LIFETIMES FOR IONS IN THE MAGNETOSPHERE

Paul H. Smith
Laboratory for Planetary Atmospheres
NASA/Goddard Space Flight Center
Greenbelt, MD 20771

N. K. Bewtra
Computer Sciences Corporation
Silver Spring, MD 20910

ABSTRACT

In applying the charge exchange mechanism to ion phenomena within the Earth's magnetosphere it is critical to the proper interpretation of observations that the charge exchange lifetimes for the ions be known as accurately as possible. Various new results have been published which significantly modify the charge exchange lifetimes which have been used in space physics research during the past decade and a half. Some of the newer results have been used in the application of the charge exchange decay mechanism but the use has been limited and for the most part incomplete. The neutral hydrogen density distribution now yields lifetimes which are shorter than previously calculated, while the functional dependence of the lifetimes on pitch angle provides for slower decay for ions mirroring off the geomagnetic equator. This review coalesces and summarizes the latest and best measurements of the physical quantities involved in the complete calculation of the charge exchange lifetime of the mirroring magnetospheric ions.

INTRODUCTION

The exosphere of atomic hydrogen surrounding the earth extends far deeper into the magnetosphere than it was believed in the early sixties. The density of atomic hydrogen has not yet been measured directly in the magnetosphere, unfortunately, and an uncertainty in our understanding of associated geophysical phenomena therefore remains with us. Fortunately, however, the neutral hydrogen density can be inferred from Lyman-alpha emission measurements (Bertaux and Blamont, 1973; Vidal-Madjar and Bertaux, 1972; Meier and Mange, 1970) or from ion mass spectrometer measurements (Brinton, 1975), coupled with the theoretical models for radial distance dependence (Johnson and Fish, 1960; Chamberlain, 1963). The derived neutral hydrogen density is large enough so that the process of charge exchange in the trapping region, where the energetic protons and heavier ions can be considered lost through the acquistion of one or more charge-neutralizing electrons from the ambient hydrogen, is a phenomenon to be seriously and exactly considered. Indeed, since the early suggestion of Dessler and Parker (1959) that the charge exchange decay mechanism could be significant in the ring current decay, arguments for and against this mechanism have been brought forth by various authors (Frank, 1967; Swisher and Frank, 1968; Prölss, 1973; Smith et al., 1976; Tinsley, 1976; Lyons and Evans, 1976). Smith et al., (1977) present several aspects of these arguments and draw conclusions about the ionic composition of the ring current based on Explorer 45 (S^3-A) observations.

In view of the importance of charge exchange decay as a loss mechanism for magnetospheric ions, this paper coalesces and summarizes what are the latest and best measurements of the physical quantities involved in the calculation of the charge exchange lifetime of the mirroring ions.

These quantities are the neutral atomic hydrogen density, the charge exchange cross section of various ions and the lifetime dependence of mirroring ions on the mirror latitude.

There are two principal relations for the charge exchange mechanism in the magnetosphere:

$$\tau_e = \frac{1}{n(r_o)\sigma v} \qquad (1)$$

where, τ_e is the mean lifetime of protons or any other ion species confined to the equatorial plane for charge exchange decay with atomic hydrogen, $n(r_o)$ is the hydrogen density in the equatorial plane, v is the velocity of the ions and σ is the charge exchange cross section of the ion with atomic hydrogen, and

$$\tau_m \approx \tau_e \cos^j \lambda_m \qquad (2)$$

where, τ_m is the charge exchange lifetime of ions mirroring off the geomagnetic equator at λ_m, the mirror latitude.

The early work by Liemohn (1961) used σ and $n(r_o)$ measurements available at that time to provide quite complete graphs for τ_e as a function of proton energy and the radial distance of the protons. He also obtained τ_m as a function of mirror latitude in the approximate form of $\tau_m = \tau_e \cos^6 \lambda_m$. Until recently, these results have been the basis for all discussions of the charge exchange mechanism in the magnetosphere, even though better measurements and theories have existed for both $n(r_o)$ and σ. Smith et al. (1976) were one of the first to use charge exchange lifetime values modified from those given by Liemohn (1961) in explaining satellite observations by using better determinations of n and σ in equation (1). Tinsley (1976)

also modified τ_e by using updated values of $n(r_o)$ and σ and Lyons and Evans (1976) used these values in explaining their observations. Smith and Bewtra (1976) made an additional step forward by recomputing the relationship between lifetimes of particles mirroring off-equator to the lifetime of particles confined to the equator (equation 2). They determined that the relationship was

$$\tau_m = \tau_e \cos^{3.5\pm0.2} \lambda_m$$

and, therefore, off-90^o pitch angles fluxes would not charge exchange decay as rapidly as was previously thought. Independently Cowley (1977) in doing a similar calculation arrived at a nearly identical conclusion.

GEOCORONAL HYDROGEN DENSITY MODELS

The neutral density distribution in a planetary atmosphere is a function of the boundary conditions at the exobase (i.e., the temperature and density distributions at the exobase). The exosphere is defined to be the region of a planetary atmosphere where the number of atomic collisions per unit time is negligible and where the controlling factors are gravitational attraction and thermal energy conducted from below. Thus below the exobase (also called the critical level) it is generally assumed that the constituents have an isotropic Maxwell-Boltzmann distribution, and above this level, in the collisionless medium, one uses Liouville's theorem to get the exospheric density as a triple integral of the distribution function over the momentum space. In this exosphere particles with an upward velocity will describe ballistic trajectories. Depending on their velocities at the exobase, they will either describe hyperbolic trajectories and escape from the atmosphere, or elliptic trajectories and return to another point on the exobase.

Johnson and Fish (1960) formulated a model for hydrogen density which had been extensively used in the sixties and early seventies for the study of magnetospheric problems. They hypothesized that in the exosphere the particle distribution corresponds to a complete Maxwellian distribution, except with certain types of hyperbolic trajectories excluded. They also assumed the conservation of escaping flux, and obtained a numerical solution to the hydrogen distribution in the exosphere. Independently, Öpik and Singer (1959, 1960, 1961) gave an analytical expression for both types of particles, elliptic and hyperbolic. Chamberlain (1963) added a third class of particles, namely, satellite

particles, created by a small number of collisions in the exosphere. In Chamberlain's terminology, these particles correspond to elliptic orbits of particles having perigee outside the critical level. Thus, these particles do not correspond to trajectories originating from within the exobase. On the other hand, the particles with elliptic orbits having perigee below the critical level rise from the critical level and eventually fall back. These are called ballistic particles. The third class of particles correspond to hyperbolic orbits and are called escaping particles. Chamberlain also considered the sources and sinks of geocoronal particles. He examined the equilibrium questions that arise because of photoionization or other loss mechanisms and related this to fixing the abundance of satellite particles. This was done by introducing the concept of a satellite critical altitude (R_{sc}). Below this altitude there exists a complete isotropic distribution of energetically allowed satellite particles, and there are no satellite particles which have a perigee above this altitude, due to the assumption that the collisional creation of satellite orbits is negligible.

The models described above correspond to an exospheric density distribution with spherical symmetry i.e., atmospheric structure is assumed uniform over the globe and there are no latitude or day-night effects. However, the interpretation of ground based, rocket and satellite experimental results often requires some degree of asymmetry in the exospheric density distribution of hydrogen (Meier 1969; Metzger and Clark, 1970). Vidal-Madgar and Bertaux (1972), McAfee (1967) and Quessette (1972) have extended Chamberlain's arguments and introduced axial asymmetries. Vidal-Madjar and Bertaux have an involved model

requiring numerical integration corresponding to any temperature and density distribution at the exobase. They derive density at a particular point in the exosphere by integrating the distribution function over the momentum part of the phase space. However, all the following discussions shall be confined to spherically symmetrical models only.

The density n(r) for the Chamberlain model is expressed in terms of density at the exobase, N_c, and a partition function, ζ, as follows:

$$n(r) = N_c \, e^{-(\lambda_c - \lambda(r))} \, \zeta(\lambda)$$

where

$$\lambda(r) = \frac{G \mu M}{k T_c r}$$

G = Gravitational constant

μ = Planetary mass

M = Atomic mass

k = Boltzman constant

T_c = Temperature at the exobase

For neutral hydrogen, λ_c can be expressed by assuming the exobase to be at 500km by

$$\lambda_c = \frac{6981.4}{T_c \text{ (in K)}}$$

and

$$\lambda(r) = \frac{1.0785 \, \lambda_c}{r \text{ (in Earth Radii)}}$$

The partition function, $\zeta(\lambda)$, can be calculated for the appropriate type of particles by integrating the distribution function with proper boundary conditions of moments. We summarize the partition functions for the ballistic, satellite and escaping particles as:

$$\zeta_{bal}(\lambda) = \frac{2}{\sqrt{\pi}}\left[\gamma(3/2,\lambda) - \frac{(\lambda_c^2 - \lambda^2)^{\frac{1}{2}}}{\lambda_c} e^{-\psi_1} \gamma(3/2,\lambda-\psi_1)\right]$$

$$\zeta_{sat}(\lambda) = \frac{2}{\sqrt{\pi}} \frac{(\lambda_c^2 - \lambda^2)^{\frac{1}{2}}}{\lambda_c} e^{-\psi_1} \gamma(3/2,\lambda-\psi_1)$$

$$\zeta_{esc}(\lambda) = \frac{1}{\sqrt{\pi}}\left[\frac{\sqrt{\pi}}{2} - \gamma(3/2,\lambda) - \frac{(\lambda_c^2 - \lambda^2)^{\frac{1}{2}}}{\lambda_c} e^{-\psi_1}\left(\frac{\sqrt{\pi}}{2} - \gamma(3/2,\lambda-\psi_1)\right)\right]$$

where $\psi_1 = \frac{\lambda^2}{\lambda + \lambda_c}$ and γ is the incomplete Γ-function (Abramowitz and Stegun, 1965).

As was stated earlier, Chamberlain introduced the concept of satellite critical altitude, R_{sc}, which will assume a role for satellite particles analogous to that of cricital level, R_c, for ballistic and escaping particles. Thus, for distances below R_{sc} there is, because of occasional collisions, a complete isotropic distribution of the satellite particles and the partition function ζ, for $r < R_{sc}$, is

$$\begin{aligned}\zeta &= \zeta_{bal} + \zeta_{sat} + \zeta_{esc} \\ &= \frac{2}{\sqrt{\pi}} \gamma(3/2,\lambda) + \zeta_{esc}(\lambda)\end{aligned} \tag{4}$$

For, $r > R_{sc}$, only those satellite particles are present which have perigees between R_c and R_{sc}. Thus, the ballistic formula can be modified as though these orbits arose from R_{sc} rather than R_c. (The ballistic or escaping components are not actually affected by this modification). Thus for $r > R_{sc}$, the partition function is

$$\zeta = \zeta_{esc}(\lambda,\lambda_c) + \zeta_{bal}(\lambda,\lambda_{cs}) \tag{5}$$

We see that $R_{sc} = R_c$ corresponds to using only equation (5) and implies no population of satellite particles. On the other hand, $R_{sc} = \infty$ corresponds to using only equation (4) and implies a complete distribution of satellite particles. A realistic situation, however, corresponds to a mixture of these cases and most Lyman-alpha measurements are adequately described by a value of $R_{sc} = 2.5R_c$ (Carruthers et al., 1976; Meier and Mange, 1970).

In Figure 1, we show the functional dependence of atomic hydrogen density on the radial distance from the center of earth as given by the Johnson and Fish (1960) model (solid line) and Chamberlain (1960) model (dashed line). A unit density at the exobase (500 km) and the value of $T_c = 1200^oK$ are assumed. Additionally, for the Chamberlain model $R_{sc} = 2.5\ R_c$ is assumed. As is obvious, the Chamberlain model gives much higher densities than the Johnson and Fish model. In Figure 2, we show the atomic hydrogen density distribution as given by the Chamberlain model for four exobase temperatures, T_c, (900^oK, 1000^oK, 1100^oK and 1200^oK). For a specific exobase temperature, a unit density at the exobase is assumed and the density distributions for 1) no satellite particle distribution, 2) partial population of satellite particles (corresponding to $R_{sc} = 2.5\ R_c$) and 3) complete satellite particle distribution are shown.

Thus, for a known atomic hydrogen density and temperature at the exobase the density at an observation point can be easily determined from these graphs.

In the absence of a simultaneous measurement of density at the exobase and the magnetospheric observation, one has to employ empirical models to derive the exobase parameters required by the Chamberlain model.

Hedin et al., (1977) have developed a global thermospheric model (MSIS model) for the neutral thermospheric composition and neutral temperature based on mass spectrometer data from five satellites (AE-B, OGO-6, San Marco-3, AEROS-A, AE-C) and incoherent scatter measurements at four ground stations (Arecibo, Jicamarca, Millstone Hill, St. Santin). The input parameters for this model are the altitude, latitude, longitude, seasonal parameters, magnetic activity parameter (Ap index), and the solar parameters (daily and average $f_{10.7}$ flux). It should be noted that the temperature and density distribution over the exobase can be represented by an approximate distribution having an axial symmetry and nearly sinusoidal variation between minimum and maximum. Thus, the average exobase temperature can be effectively approximated by $\frac{1}{2}$ $(T_{max} + T_{min})$. It is worth pointing out that the hydrogen density distribution is inverse in phase with the temperature. Thus, the actual variation of the atomic hydrogen (see Figure 2) in the magnetosphere is greatly reduced. Vidal-Madjar et al. (1974) have parameterized the atomic hydrogen density and temperature at the exobase based on the OSO- 5 solar Lyman alpha measurements. They provide in a tabular form for the years 1969 to 1971, the daily exobase temperature (including minimum and maximum) and the atomic hydrogen density as well as the fit through their data showing relationship between exobase temperature and the density. In Figure 3, we show the actual range in the atomic hydrogen density variation in the magnetosphere for a variation in exobase temperature of $900^{o}K$ to $1200^{o}K$ and the corresponding variation in the density of 4×10^{4} cm^{-3} to 1.1×10^{5} cm^{-3}.

CHARGE EXCHANGE CROSSSECTION MEASUREMENTS

As was stated earlier, energetic protons and heavier ions can be lost from the trapping regions through acquisition of charge-neutralizing electrons from the ambient neutral hydrogen surrounding the earth. This is the charge exchange process. Charge exchange lifetimes are sufficiently short at the ring current energies that this process is an important loss mechanism for these ions. In this section, we shall summarize the survey of cross sections, measured and theoretically derived, for the following collision processes:

$$H^+ + H \longrightarrow H + H^+ \qquad (a)$$

$$H_e^{++} + H \longrightarrow He^+ + H^+ \qquad (b)$$

$$He^+ + H \longrightarrow He + H^+ \qquad (c)$$

$$O^+ + H \longrightarrow O + H^+ \qquad (d)$$

In these interactions, it is assumed that each member of the colliding pair is in its ground state and the final products may be in the ground state or in an excited state. Momentum and energy transfer during charge exchange are negligible, i.e., the incident particle leaves the collision with essentially unchanged energy but a changed charge state. This is true whenever the incident energy is large compared with excitation and ionization energies, which are of the order of a few eV. It is also important to point out that for many charge exchange cross section experiments, molecular hydrogen was used rather than atomic hydrogen as the target. In all the following discussions, the cross sections have been properly normalized to atomic hydrogen as the target.

H^+ on H

Cross sections for reaction (a) at low energies (less than 50 keV)

were first measured by Fite et al. (1960) and used extensively in early work on the studies of ring current particle loss. The best experimental measurements available for the low energy region are those of McClure, (1976) in the energy range of 2-117 keV. He used a heated target chamber containing mostly dissociated hydrogen gas. His estimated error is ±5% after correcting for the presence of molecular hydrogen in the target gas. Several theoretical calculations (Mapelton, 1962; Bates and Dalgarno, 1953; Dalgarno and Yadav, 1953) agree with his measurements over different parts of the energy range. Fite et al. (1960) used a crossed beam experiment and their measurements should provide the cross section reliably in the low energy end (less than 10 keV). Stier and Barnett (1956) provided the experimental data for the energy range 120 to 200 keV using a molecular hydrogen target and give an estimated error of ±5%. For completeness, the best data for high energies were provided by Toburen et al. (1968) in the energy range 200 keV to 1 MeV with an error estimate of ±10%. These values are summarized in Table 1.

He^{++} on H

Fite et al. (1962) provided the experimental results for reaction (b) in the energy range 100 eV to 32 keV using an atomic hydrogen target. They used modulated crossed beams and the isotope ^3He in order to differentiate the charge to mass ratio for He^{++} and H_2^+. At the low energy, data are good to within ±25% with the error decreasing to about ±13% at high energies. They normalized their data to the charge exchange cross sections for protons on atomic hydrogen at each energy. Shah and Gilbody (1974) have provided the best measurements for this reaction in the energy range 6 to 60 keV by the passage of $^3He^{++}$ ions through a tungsten tube

TABLE 1. Charge Exchange Cross Section for $H^+ + H \rightarrow H + H^+$. See text for source of measurement.

Energy (keV)	Cross Section (cm^2)
1.92	13.3×10^{-16}
3.04	12.1×10^{-16}
3.82	11.1×10^{-16}
4.8	10.5×10^{-16}
6.05	9.85×10^{-16}
9.6	8.6×10^{-16}
12.1	7.5×10^{-16}
19.2	5.0×10^{-16}
30.4	2.97×10^{-16}
38.2	1.86×10^{-16}
48.0	1.10×10^{-16}
60.5	6.0×10^{-17}
76.2	3.0×10^{-17}
100.0	1.24×10^{-17}
117.5	6.4×10^{-18}
120.0	6.6×10^{-18}
140.0	3.7×10^{-18}
160.0	3.7×10^{-18}
180.0	1.4×10^{-18}
200.0	8.8×10^{-19}

furnace containing highly dissociated hydrogen and observed He^+ ions in all final capture states. They estimate an uncertainty of 8 to 10%. In general, the cross sections obtained by Fite et al. (1962) are much lower than those of Shah and Gilbody (1974). The Fite et al. (1962) data for reaction (b) was renormalized by Shah and Gilbody (1974) to the cross section for reaction (a) as measured by McClure (1966). These values then show reasonable agreement to the similar cross sections measured by Shah and Gilbody (1974).

Several theoretical calculations have been done for reaction (b). Basu et al. (1967) and Malaviya (1969) obtained n=2 capture cross sections by considering four final states of He^+. Rapp (1973, 1974) has performed the most complete calculation for capture and excitation in reaction (b) and has considered 11 final states. These calculations show good agreement with earlier mentioned measurements, particularly in the 10 to 60 keV incident $^4He^{++}$ energy region.

It may be worth noting that most experimental cross sections are based on the mass 3 isotope of He^{++}, while most theoretical cross sections are for the more abundant isotope corresponding to mass 4. Assuming the scaling of the cross section, that is, the cross section depending on the velocity of the incident ions, it is a linear shift in the energy scale of the cross section for one isotope compared to the cross section for the other isotope. We shall be discussing the isotope corresponding to mass 4. Table 2 gives cross sections for reaction (b) as determined from a smooth line which we constructed through the data values obtained by Shah and Gilbody (1974) and the renormalized Fite et al. (1962) values.

TABLE 2. Charge Exchange Cross Section for $^4He^{++} + H \rightarrow {}^4He^{+} + H^{+}$. See text for source of measurements.

Energy (keV)	Cross Section (cm^2)
5.5	3.5×10^{-16}
8.0	5.5×10^{-16}
12.0	7.2×10^{-16}
16.0	8.4×10^{-16}
26.0	12.0×10^{-16}
40.0	12.0×10^{-16}
52.0	11.2×10^{-16}
65.0	10.5×10^{-16}
80.0	9.0×10^{-16}

He^+ on H

Allison (1958) and Barnett and Stier (1958) have provided the measurements for this cross section at low energies and high energies, respectively. Allison and Garcia-Munoz (1962) have provided a report on the results of Allison (1958) and Barnett and Stier (1958). All measurements of this cross section have been with molecular hydrogen, so that results at lower energies will be relatively inaccurate. A possibility exists that the cross section for reaction (c) can be obtained by applying the principle of detailed balance on the inverse reaction: $H^+ + He \rightarrow H + He^+$. However, the capture of He^+ into an excited state for reaction (c) can be comparable to the capture into the ground state in certain energy ranges. Consequently, the inferred cross section may not be accurate. In Table 3 the cross sections for reaction (c) which we obtained by a best fit of the values of Allison (1958) and Barnett and Stier (1958) are listed.

O^+ on H

Fite et al. (1962) have made the only measurement of the cross section for reaction (d) using a modulated crossed beam technique. However, in their experiment, the energy range of the incident O^+ ions was 30 eV to 10 keV. Above this energy they have provided an empirical formula in a form which is characteristic of resonance behavior; the reaction (d) falls in this category due to the approximate energy balance. Fite et al. (1962) use the cross section of reaction (a) at the incident ion energy of 1.9 keV to normalize the experimental data for reaction (d). As stated earlier, better measurements (McClure, 1966) for reaction (a) exist now, and this requires that the measurements of Fite et al. (1962) and their empirical formula be properly renormalized.

TABLE 3. Charge Exchange Cross Section for $^4He^+ + H \rightarrow {}^4He + H^+$. See text for source of measurement.

Energy (keV)	Cross Section (cm^2)
4.0	3.6×10^{-18}
8.0	4.7×10^{-18}
14.0	6.7×10^{-18}
20.0	8.2×10^{-18}
26.0	9.6×10^{-18}
40.0	11.6×10^{-18}
50.0	12.3×10^{-18}
60.0	13.0×10^{-18}
70.0	13.0×10^{-18}
80.0	12.0×10^{-18}
100.0	10.8×10^{-18}
120.0	9.2×10^{-18}
140.0	7.7×10^{-18}
160.0	6.4×10^{-18}
180.0	5.6×10^{-18}
200.0	4.9×10^{-18}

We renormalized these values and they are shown in Table 4 for incident energies up to 25 keV. At higher ion energies, however, the predicted cross section becomes unreliable. A better estimate of the cross section at these energies can be obtained by using the principle of detailed balancing on the reverse reaction.

$$H^+ + O \rightarrow H + O^+ \qquad (e)$$

If we define by σ_d the cross section for the direct reaction and by σ_r the cross section of the reverse reaction (at same center of mass velocity), it can be shown (Mapelton, 1972) that

$$(2S_f + 1)(2L_f + 1)\sigma_r = 2(2S_i + 1)(2L_i + 1)\sigma_d$$

where L_i and L_f are the initial and final orbital angular momentum and S_i and S_f are the initial and final spin momentum. If we assume that the atomic oxygen, which is in the ground state ^3P, ionizes to the ground state of O^+ ions (namely, ^4S state), it can be easily seen that

$$\sigma_d(O^+(^4S) + H \rightarrow O(^3P) + H^+) = 9/8\sigma_r(H^+ + O(^3P) \rightarrow H + O^+(^4S)).$$

Stebbings et al. (1964) have measured the cross section for reaction (e). Stier and Barnett (1956) have also measured this cross section, using molecular oxygen, with lower uncertainties. We have used these measurements and the principle of detailed balance to obtain the cross section for reaction (d) at O^+ energies greater than 25 keV, and these are shown in Table 4.

In Figure 4, we summarize the results for reactions (a), (b), (c), and (d) by plotting the 'normalized lifetime' i.e., $\frac{1}{\sigma v}$ for various ions in the energy range 1 to 200 keV.

TABLE 4. Charge Exchange Cross Section for the Reaction $O^+ + H \rightarrow O + H^+$. See text for source of measurement

Energy (keV)	Cross Section (cm^2)
1.0	7.82×10^{-16}
5.0	6.10×10^{-16}
10.0	5.61×10^{-16}
25.0	5.01×10^{-16}
64.0	5.5×10^{-16}
80.0	5.29×10^{-16}
112.0	5.06×10^{-16}
44.0	4.84×10^{-16}
92.0	4.33×10^{-16}

DEPENDENCE OF CHARGE EXCHANGE LIFETIME ON MIRROR LATITUDE

The dependence of the charge exchange lifetimes on the mirror latitude had been considered by Liemohn (1961) based on Johnson and Fish (1960) hydrogen density models. He obtained an empirical fit in the form of equation (2) with j=6. Since then, most of the researchers have been using these values to compare with their observations. Prölss (1973) used a better hydrogen density model and speculated that j=5 would yield a better approximation. Smith and Bewtra (1976) and independently Cowley (1977) examined in detail the lifetime of mirroring particles and recomputed the relationship using the Chamberlain (1963) model of neutral hydrogen density.

Smith and Bewtra (1976) and Cowley (1977) both considered that ions bouncing between the mirror points make a large number of bounces before charge exchanging with neutral hydrogen. Thus the instantaneous hydrogen density over a mirror path can be effectively averaged to get the time averaged density, $\bar{n}$, that the particle encounters as

$$\bar{n} = \frac{\int_{\lambda=0}^{\lambda_m} n(r) \frac{1}{v_{\parallel}(r)} ds}{\int_{\lambda=0}^{\lambda_m} \frac{1}{v_{\parallel}(r)} ds} \qquad (6)$$

Using equation (1), then, $\tau_m/\tau_e = n_e/\bar{n}$ and the ratio τ_m/τ_e can be computed by calculating the integrals in equation (6). Smith and Bewtra (1976)

determined that, for $T_c = 1000^oK$, $R_{sc} = 2.5R_c$ and at L = 4, a least squares fit of the calculated ratio, τ_m/τ_e, to a function of the form $\cos^j\lambda_m$ yielded a value of j = 3.4. Cowley (1977) also determined j to be in the range 3 to 4.

The ratio τ_m/τ_e is independent of N_c, the density at the exobase, but does depend on the two other parameters, T_c and R_{sc}, of the Chamberlain model. Smith and Bewtra (1976) computed the effect on this ratio of varying the two parameters. In fitting the ratio using various extreme combinations they found, for T_c between 900^oK and 1200^oK, for R_{sc} between $2.25R_c$ and $2.75R_c$, and for L-values between 2.5 and 10, that j fell in the range $j = 3.5 \pm 0.2$.

Cowley (1977) additionally suggested the use of an alternative approximation of the form

$$\frac{\tau_m}{\tau_e} = \left[\cos\left(\frac{\pi}{2}\,\frac{\lambda_m}{\Lambda}\right)\right]^{\gamma_3} \qquad (7)$$

where Λ is the latitude at which the field line ($\cos^2\Lambda = 1/L$) intersects the Earth's surface. He provides tabulations of γ_3 for various L-values, T_c values and R_{sc} values. He concluded that the alternative approximation (eq. 7) gave good values of τ_m/τ_e over a large λ_m range and even better approximations than $\cos^j\lambda_m$ and other functional forms which he tried.

It is worth pointing out that at a mirror latitude of 35^o the charge exchange lifetime using j = 3.5 is a factor of 2 longer than predicted by the Liemohn (1961) results. Another way of looking at this difference

is that using the new lifetime for protons of energy 10 keV mirroring at a latitude of 35^{o}, the flux after 1 day will be a factor of 15 higher than that predicted by Liemohn's results.

SUMMARY

In this paper we started with the two principal relations for charge exchange lifetimes. Figure 2 summarizes the normalized atomic hydrogen distribution as a function of radial distance using the Chamberlain model for a range of exobase temperatures and for various combinations of satellite particles. Thus, if the atomic hydrogen density at the exobase is known, one can determine the density at any point of observation. In general, the temperature and density at the exobase are functions of several geophysical parameters. Therefore, in Figure 3 we have shown the range in the actual density distribution for several magnetic storms during the early life of Explorer 45 in the period December, 1971 to May, 1972, assuming the satellite particle distribution to be described by the generally accepted relationship $R_{sc} = 2.5R_c$. Figure 4 summarizes the cross section measurements for various ions in the energy range 1 keV to 200 keV in the form of normalized charge exchange lifetimes $(\frac{1}{\sigma v})$. Thus, using these figures the equatorial lifetimes can be determined for any of these ions at a specific energy and L-value. The charge exchange lifetime for the mirroring particles with a specific mirror latitude can be determined by $\tau_m = \tau_e \cos^{3.5 \pm 0.2}\lambda_m$ or by using equation (7).

The results of this paper are based on our current knowledge of the planetary atmosphere neutral hydrogen distribution and the charge exchange cross sections for various ions. The charge exchange lifetimes of the equatorial particles are much shorter and the dependence on mirror latitude is much weaker than the Liemohn (1961) results. Thus, we recommend that the ionic composition of the ring current during the recovery phase of

magnetic storms should be re-examined in light of these current results.

To highlight this conclusion, we show, as an example, how these results affect the particle flux decay as a function of mirror latitude. Assuming at time t=o, an isotropic and unit flux distribution for 10 keV O^+ and H^+ ions at L = 4, and assuming geophysical parameters corresponding to the February 24, 1972 magnetic storm, we show in Figure 5 the mirror latitude distributions as predicted by the new lifetime values after time periods which are multiples of 7.8 hours (roughly the orbital period for Explorer 45). The dotted lines show the distribution predicted by using Liemohn's mirror latitude dependence of $\tau_m = \tau_e \cos^6\lambda_m$ and the solid lines correspond to the dependence of $\tau_m = \tau_e \cos^{3.5}\lambda_m$; for both cases the equatorial lifetimes, τ_e, are the new values summarized in this paper.

It is clear that the flux distributions as a function of mirror latitude decay much slower using the new functional dependence. Two additional points are also evident from this figure. First, assuming comparable initial fluxes, the O^+ ions after about one day would exhibit a pitch angle distribution significantly separated from the H^+ ions which would have more rapidly decayed. This can aid in the determination of ion composition in the ring current. Second, the loss cone for these particles is about 60^o mirror latitude and, therefore, these distributions will be quite flat with sharp cut-offs near the loss cone for many hours after on initial isotropic distribution. Obviously the ions with longer equatorial lifetimes (eq. O^+ and He^+) will exhibit this shape for a longer time.

With these new lifetime values it will be indeed a challenge to

re-examine some of the previous results, and exciting to interpret the new measurements and to gain a more complete understanding of our ring current environment.

ACKNOWLEDGEMENT

The authors wish to thank their colleague R. A. Hoffman for his suggestions and critical comments on this review.

REFERENCES

Abramowitz, M., and J. A. Stegun, Handbook of Mathematical Functions, National Bureau of Standards Applied Mathematics Series, U. S. Government Printing Office, Washington, D. C., 1965.

Allison, S. K., Experimental results on charge changing collisions of hydrogen and helium atoms and ions at kinetic energies above 0.2 keV, Rev. Mod. Phys., 30, 1137, 1958.

Allison, S. K., and M. Garcia-Munoz, Electron capture and loss at high energies, Atomic and Molecular Processes, ed. D. R. Bates, Academic Press, 1962.

Barnett, C. F., and P. M. Stier, Charge exchange cross section for helium ions in gases, Phys. Rev., 109, 385, 1958.

Basu, D., P. M. Bhattacharya, and G. Chatterjee, Electron capture by alpha particle incident on atomic hydrogen, Phys. Rev., 163, 8, 1967.

Bates, D. R., and A. Dalgarno, Electron capture - III; Capture into excited states in encounters between hydrogen atoms and fast protons, Proc. Phys. Soc. (London), A66, 972, 1953.

Bertaux, J. L., and J. E. Blamont, Interpretation of OGO-5 Lyman alpha measurements in the upper geocorona, J. Geophys. Res., 78, 80-91, 1973.

Brinton, H. C., H. G. Mayr, and W. E. Potter, Winter bulge and diurnal variation in hydrogen inferred from AE-C composition measurements, Geophys. Res. Lett., 2, 389-392, 1975.

Carruthers, G. R., T. Page, and R. R. Meier, Apollo 16 Lyman alpha imagery of the hydrogen geocorona, J. Geophys. Res., 81, 1664-1672, 1976.

Chamberlain, J. W., Planetary coronal and atmospheric evaporation, Planet. Space Sci., 11, 901, 1963.

Cowley, S. W. H., Pitch angle dependence of the charge exchange life time of ring current ions, Planet. Space Sci., 25, 385-393, 1977.

Dalgarno, A., and H. N. Yadav, Electron capture II: Resonance capture from hydrogen atoms by slow protons, Proc. Phys. Soc. A, 66, 173, 1953.

Dessler, A. J., and E. N. Parker, Hydromagnetic theory of geometric storms, J. Geophys. Res., 64, 2239, 1959.

Fite, W. L., A. C. H. Smith, and R. F. Stebbings, Charge transfer in collisions involving symmetric and asymmetric resonance, Proc. Roy. Soc. London A, 268, 527, 1962.

Fite, W. L., R. F. Stebbings, D. G. Hummer, and R. T. Brachmann, Ionization and charge transfer in proton-hydrogen atom collisions, Phys. Rev., 119, 663-668, 1960.

Frank, L. A., On the extraterrestrial ring current during geomagnetic storms, J. Geophys. Res., 72, 3753-3767, 1967.

Hedin, A. E., C. A. Reber, G. P. Newton, N. W. Spencer, H. C. Brinton, H. G. Mayr, and W. E. Potter, A global thermospheric model based on mass spectrometer and incoherent scatter data, MSIS 2, Composition, J. Geophys. Res., 82, 2148-2156, 1977.

Hedin, A. E., J. E. Salah, J. V. Evans, C. A. Reber, G. P. Newton, N. W. Spencer, D. C. Kayser, D. Alcayde, P. Bauer, L. Cogger, and J. P. McClure, A global thermospheric model based on mass spectrometer and incoherent scatter data: MSIS, 1, N_2 Density and temperature, J. Geophys. Res., 82, 2139-2147, 1977.

Johnson, F. S., and R. A. Fish, The telluric hydrogen corona, Astrophys. J. 131, 502-515, 1960.

Liemohn, H., The lifetimes of radiation belt protons with energies between 1 keV and 1 MeV, J. Geophys. Res., 66, 3593-3595, 1961.

Lyons, L. R., and D. S. Evans, The inconsistency between proton charge exchange and the observed ring current decay, J. Geophys. Res., 81, 6197-6200, 1976.

Malaviya, V., Resonance charge transfer in $He^{2+} - H^{(1s)}$ collisions, J. Phys. B (London), 2, 843, 1969.

Mapleton, R. A., Electron capture from atomic hydrogen by protons, Phys. Rev., 126, 1477, 1962.

Mapleton, R. A., Theory of Charge Exchange, John Wiley and Sons, Inc. 1972.

McAfee, J. R., Lateral flow in the exosphere, Planet. Space Sci., 15, 599, 1967.

McClure, G. W., Electron transfer in proton-hydrogen-atom collisions: 2-117 keV, Phys. Rev., 148, 47-54, 1966.

Meier, R. R., Balmer alpha and Lyman beta in the hydrogen geocorona, J. Geophys. Res., 74, 3561, 1969.

Meier, R. R., and P. Mange, Geocoronal hydrogen: An analysis of the Lyman alpha airglow observed from OGO-4, Planet. Space Sci., 18, 803-821, 1970.

Meier, R. R., and P. Mange, Spatial and temporal variations of the Lyman alpha airglow and related atomic hydrogen distributions, Planet. Space Sci., 21, 304-327, 1973.

Metzger, P. H., and M. A. Clark, On the diurnal variation of the exospheric neutral hydrogen temperature, J. Geophys. Res., 75, 5587, 1970.

Öpik, E. J., and S. F. Singer, Distribution of density in a planetary exosphere, Phys. Fluids, 2, 653, 1959.

Öpik, E. J., and S. F. Singer, Distribution of density in a planetary exosphere, Phys. Fluids, 3, 486, 1960.

Öpik, E. J., and S. F. Singer, Distribution of density in a planetary exosphere II, Phys. Fluids, 4, 221, 1961.

Prölss, G. W., Decay of the magnetic storm ring current by the charge-exchange mechanism, Planet. Space Sci., 21, 983-992, 1973. Quessette, J. A., Atomic hydrogen densities at the exobase, J. Geophys. Res.

Rapp, D., Electron Transfer and excitation in collisions of He^{++} with H., J. Chem. Phys., 58, 2043, 1973.

Rapp, D., Electron capture and excitation in collisions of He^{++} with H. II Convergence of the atomic expansion, J. Chem. Phys., 61, 3777-3779, 1974.

Shah, M. B., and H. B. Gilbody, Charge transfer in He^{++}-H collisions in the energy range 6-60 keV, J. Phys. B: Atom. Molec. Phys., 7, 256-268, 1974.

Smith, P. H., and N. K. Bewtra, Dependence of the charge exchange lifetimes on mirror latitude, Geophys. Res. Lett., 3, 689-692, 1976.

Smith, P. H., R. A. Hoffman, and T. A. Fritz, Ring current proton decay by charge exchange, J. Geophys. Res., 81, 1976.

Smith, P. H., N. K. Bewtra, and R. A. Hoffman, Inference of the ring current ion composition by means of charge exchange decay, (to be submitted to), J. Geophys. Res., 1977.

Stebbings, R. F., A. C. H. Smith, and H. Ehrhardt, Charge transfer between oxygen atoms and O^+ and H^+ ions, Atomic Collision Processes, ed. M. R. C. McDowell, North-Holland Publishing Company, 1964.

Stier, P. M., and C. F. Barnett, Charge exchange cross sections of hydrogen ions in gases, Phys. Rev., 103, 896, 1956.

Swisher, R. L., and L. A. Frank, Lifetimes of low-energy protons in the outer radiation zone, J. Geophys. Res., 73, 5665-5672, 1968.

Tinsley, B. A., Evidence that the recovery phase ring current consists of helium ions, J. Geophys. Res., 81, 6193-6196, 1976.

Toburen, L. H., M. Y. Nakai, and R. A. Langley, Measurement of high-energy charge-transfer cross sections for incident protons and atomic hydrogen in various gases, Phys. Rev., 171, 114, 1968.

Vidal-Madjar, A., and J. L. Bertaux, A calculated hydrogen distribution in the exosphere, Planet. Space Sci., 20, 1147-1162, 1972.

Vidal-Madjar, A., J. E. Blamont, and B. Phissamay, Evolution with solar activity of the atomic hydrogen density at 100 kilometers of altitude J. Geophys. Res., 79, 233-241, 1972

FIGURE CAPTIONS

Figure 1. Functional dependence of atomic hydrogen density on the radial distance from the center of earth as given by Johnson and Fish model (shown as dashed line) and the Chamberlain model (shown as solid line). A unit density and temperature of 1200^{o}K at the exobase Tc are assumed. For Chamberlain model, values of $R_{sc} = 2.5\ R_c$ is used.

Figure 2: Functional dependence of atomic hydrogen density distribution as given by the Chamberlain model for a range of exobase temperature. Panels (a), (b), (c) and (d) correspond to T_c = 900^{o}K, 1000^{o}K, 1100^{o}K and 1200^{o}K respectively. For each panel, dashed line corresponds to all satellite particles included, solid line corresponds to partial population of satellite particles ($R_{sc} = 2.5\ R_c$), and dash-dotted line corresponds to no satellite present. Unit density at the exobase is assumed.

Figure 3: Change in neutral hydrogen density as a function of radial distance (in Earth radii). Variation in exobase temperature, T_c, of 900^{o}K to 1200^{c}K, and in density of $4 \times 10^{4} cm^{-3}$ to $1.1 \times 10^{5} cm^{-3}$ is assumed.

Figure 4: Normalized charge exchange lifetimes ($1/\sigma v$) in seconds per cm^3 for various ions in the incident energy range of 1 to 200 keV.

Figure 5: Evolution in pitch angle distribution as a function of mirror latitude for charge exchange decay, starting with a unit isotropic distribution at time t = 0. Each panel corresponds to a time interval of 7.8 hours. Solid lines show the decay as predicted by $\tau_m/\tau_e = \cos^{3.5}\lambda_m$ dependence and dotted line shows the decay as predicted by $\tau_m/\tau_e = \cos^{6}\lambda_m$ dependence.

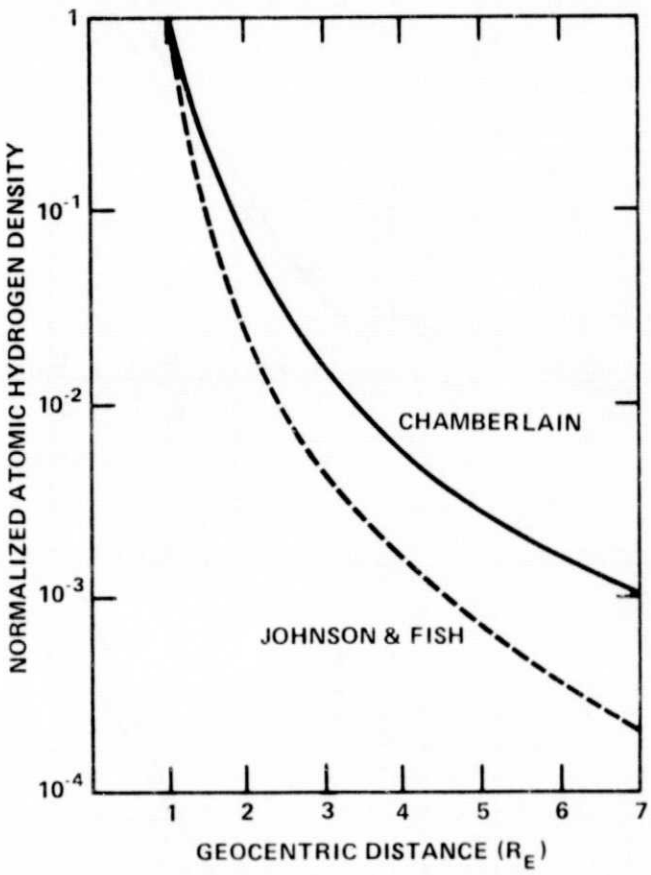
NORMALIZED ATOMIC HYDROGEN DENSITY
1
10^{-1}
10^{-2}
10^{-3}
10^{-4}
CHAMBERLAIN
JOHNSON & FISH
1
2
3
4
5
6
7
GEOCENTRIC DISTANCE (R_E)

FIGURE 1

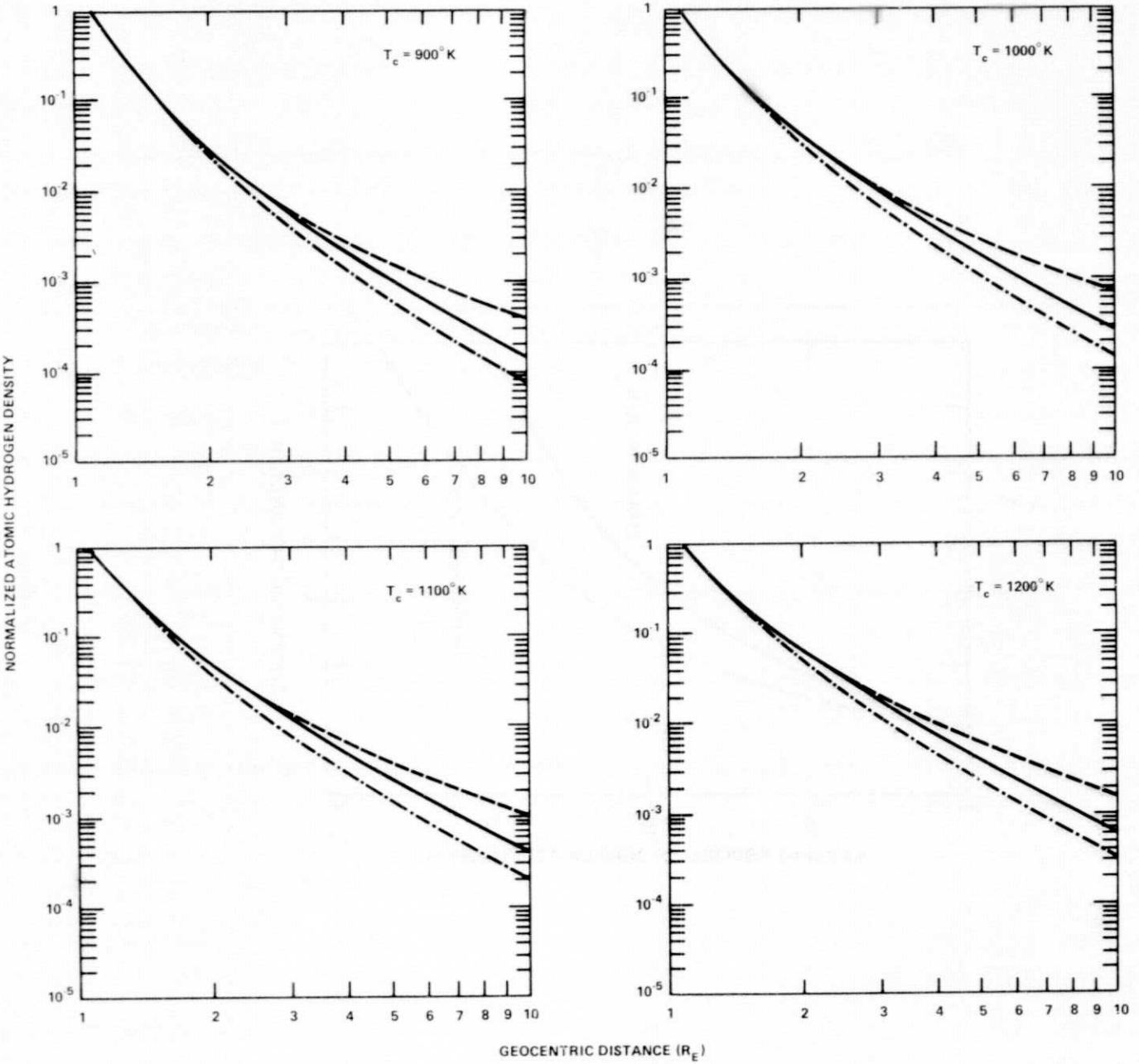
T_c = 900° K
T_c = 1000° K
T_c = 1100° K
T_c = 1200° K
NORMALIZED ATOMIC HYDROGEN DENSITY
GEOCENTRIC DISTANCE (R_E)

FIGURE 2

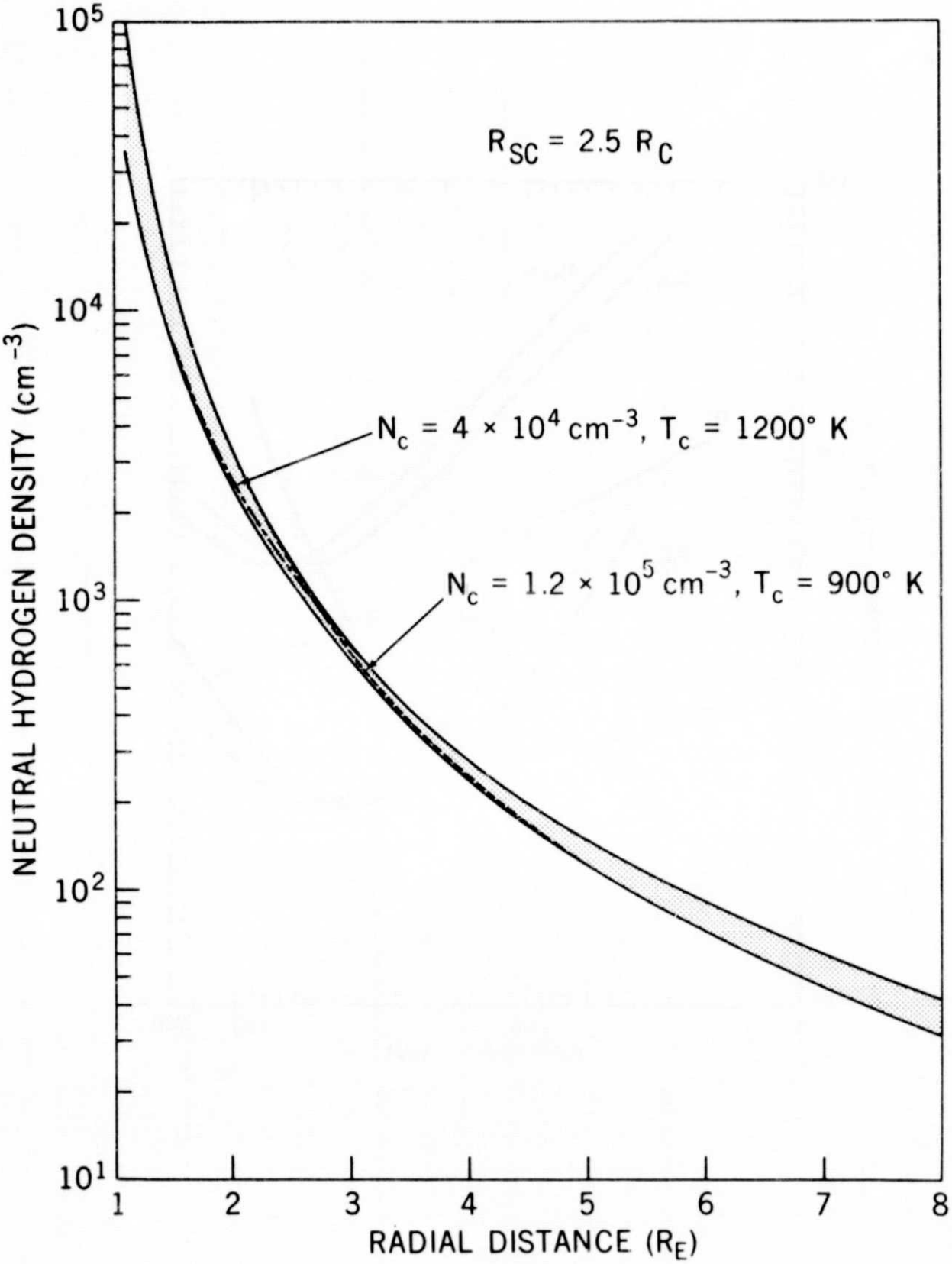
10^5
10^4
10^3
10^2
10^1
NEUTRAL HYDROGEN DENSITY (cm^{-3})
$R_{SC} = 2.5\ R_C$
$N_c = 4 \times 10^4\ cm^{-3}$, $T_c = 1200°\ K$
$N_c = 1.2 \times 10^5\ cm^{-3}$, $T_c = 900°\ K$
1
2
3
4
5
6
7
8
RADIAL DISTANCE (R_E)

FIGURE 3

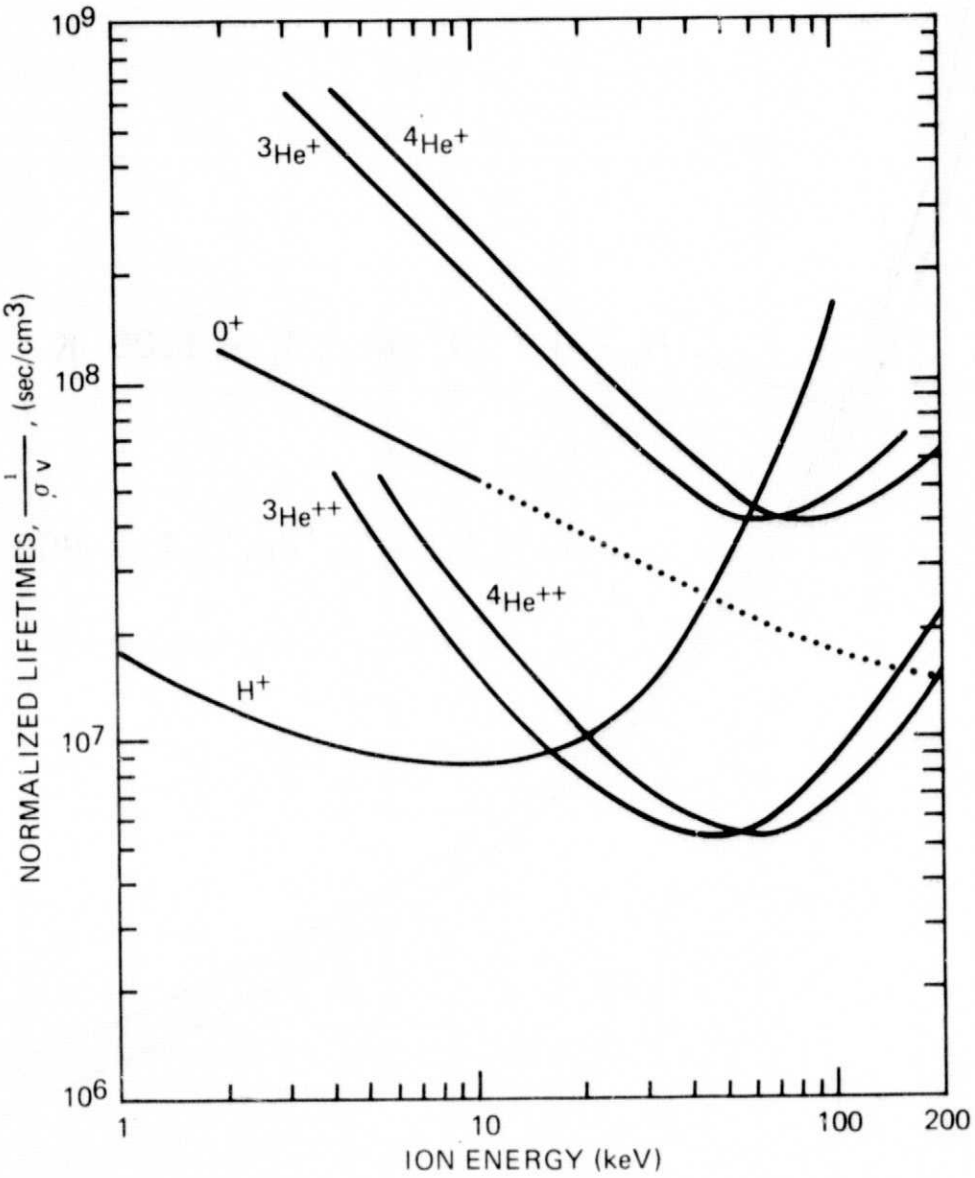
10^9
10^8
10^7
10^6
NORMALIZED LIFETIMES, $\frac{1}{\sigma v}$, (sec/cm^3)
$^3He^+$
$^4He^+$
0^+
$^3He^{++}$
$^4He^{++}$
H^+
1
10
100
200
ION ENERGY (keV)

FIGURE 4

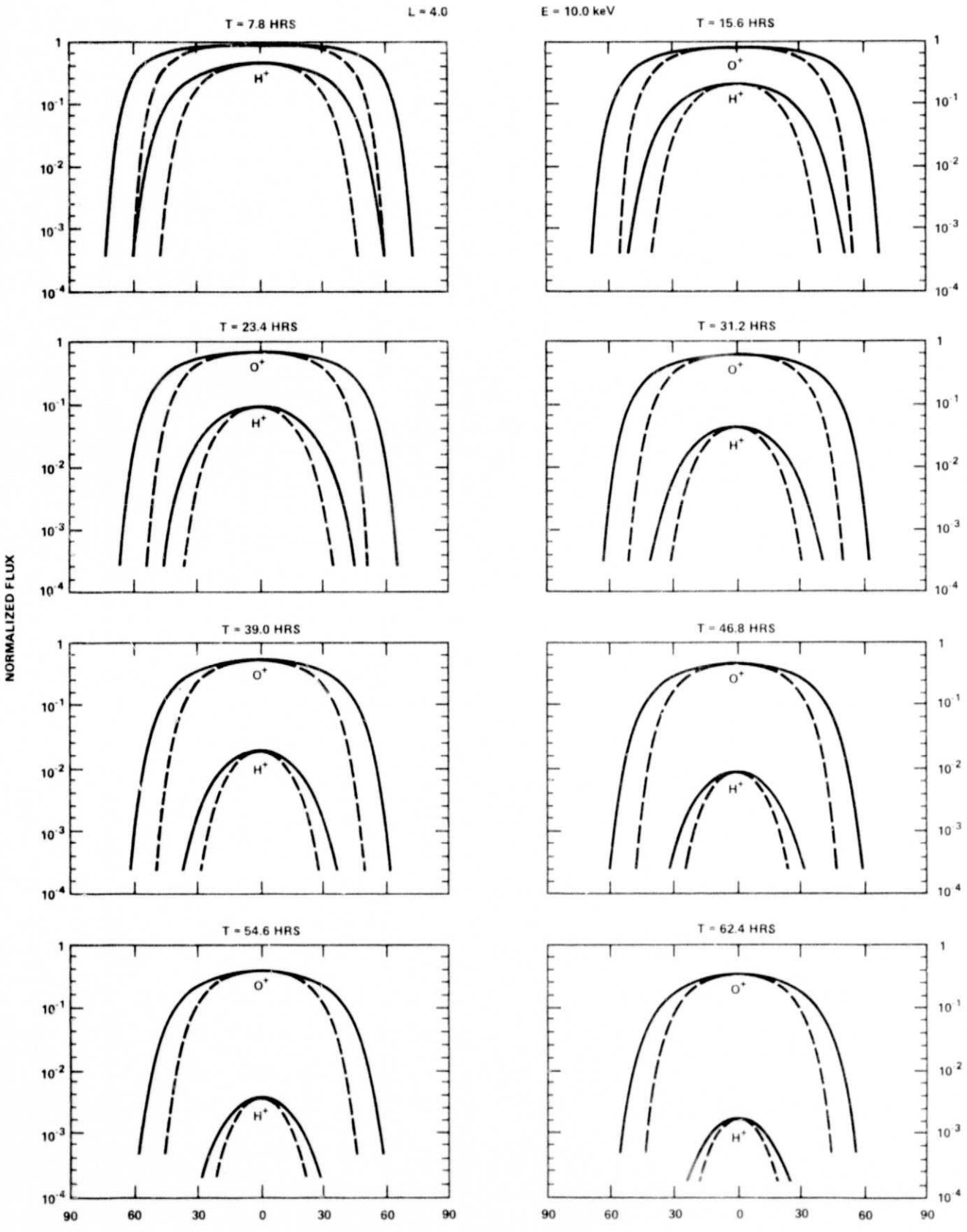
PITCH ANGLE DISTRIBUTIONS FOR CHARGE EXCHANGE DECAY
L = 4.0
E = 10.0 keV
T = 7.8 HRS
T = 15.6 HRS
T = 23.4 HRS
T = 31.2 HRS
T = 39.0 HRS
T = 46.8 HRS
T = 54.6 HRS
T = 62.4 HRS
O+
H+
NORMALIZED FLUX
1
10-1
10-2
10-3
10-4
90
60
30
0
30
60
90
MIRROR LATITUDE (DEGREES)

FIGURE 5